General Disclaimer

One or more of the Following Statements may affect this Document

- This document has been reproduced from the best copy furnished by the organizational source. It is being released in the interest of making available as much information as possible.

- This document may contain data, which exceeds the sheet parameters. It was furnished in this condition by the organizational source and is the best copy available.

- This document may contain tone-on-tone or color graphs, charts and/or pictures, which have been reproduced in black and white.

- This document is paginated as submitted by the original source.

- Portions of this document are not fully legible due to the historical nature of some of the material. However, it is the best reproduction available from the original submission.

LSA Project Task Report

5101-56

DOE/JPL-1012-78/3
Distribution Category UC-63

Structure of Deformed Silicon and Implications for Low Cost Solar Cells

Prepared for

Department of Energy

by

Jet Propulsion Laboratory
California Institute of Technology
Pasadena, California

(JPL PUBLICATION 78-13)

Prepared by the Jet Propulsion Laboratory, California Institute of Technology, for the Department of Energy by agreement with the National Aeronautics and Space Administration.

The JPL Low-Cost Solar Array Project is sponsored by the Department of Energy (DOE) and forms part of the Solar Photovoltaic Conversion Program to initiate a major effort toward the development of low-cost solar arrays.

LSA Project Task Report

5101-56

DOE/JPL-1012-78/3
Distribution Category UC-63

Structure of Deformed Silicon and Implications for Low Cost Solar Cells

N. Mardesich
M. H. Leipold
G. B. Turner
T. G. Digges, Jr.

March 1, 1978

Prepared for
Department of Energy
by
Jet Propulsion Laboratory
California Institute of Technology
Pasadena, California
(JPL PUBLICATION 78-13)

CONTENTS

Figures

Table

NOTE

N. Mardesich is presently with Spectrolab, Sylmar, California.

ABSTRACT

The microstructure and minority carrier lifetime of silicon were investigated in uniaxially compressed silicon samples. The objective of the investigation was to determine if it is feasible to produce silicon solar cells from sheet formed by high temperature rolling. The initial structure of the silicon samples ranged from single crystal to fine-grained polycrystals. The samples had been deformed at strain rates of 0.1 to 8.5 sec^{-1} and temperatures of 1270-1380°C with subsequent annealing at 1270-1380°C.

Recrystallization was incomplete even after long anneals. A 10 hour anneal of fine-grained samples with as much as 51% strain only caused 95% of the samples to recrystallize and even then the recrystallized grains contained twin boundaries and dislocations. The recrystallization in the large grained samples was also incomplete and further, it has been shown that large grained material cracks readily during significant deformation (up to 40%). The major mode of recrystallization appears to be migration of existing boundaries into the deformed regions. Minority carrier diffusion length was drastically reduced by deformation and recovered only slightly with annealing. These results suggest that high temperature rolling of silicon to produce sheet for solar cells of high efficiency is not practical.

I. INTRODUCTION

Silicon is a material with potential for low cost photovoltaic energy conversion. One possible method to form silicon sheet material which can then be converted into solar cells is hot rolling. Investigations have demonstrated that high temperature deformation is possible[1]. However, there remain questions as to whether the structure of the recrystallized material will permit the fabrication of high efficiency solar cells.

The most important figure of merit for silicon to be used in solar cells is the effective minority carrier diffusion length (L_d)[2] which depends on both grain size and intragrain diffusion length. Investigators[3-6] have demonstrated that effective diffusion lengths in the range of 30 μm minimum are necessary for high efficiency solar cells (>12%), while shorter effective diffusion lengths are indicative of lower efficiencies. Several investigators have shown that effective diffusion length is no larger than the grain size and may be substantially less[2,7,8]. High efficiency cells, then, require grains larger than 30 μm. In addition, structure within the grains may limit the intragrain diffusion length and hence the effective diffusion length. Many large grain ribbon materials, which have intersecting twin planes and dislocations, also have short diffusion lengths[3-6] and low efficiencies.

The purpose of this paper is to describe the structure of recrystallized silicon and its behavior with respect to deformation rates and annealing cycles. The paper further assesses the implications of recrystallized structure on high efficiency solar cells and cost.

II. SAMPLE PREPARATION

A variety of starting grain sizes and structures was investigated. Large single crystals as well as 1 mm grain size polycrystals were obtained from the Czochralski growth process. Fine-grained polycrystals were obtained from the chemical vapor deposition (CVD) process. Samples, for which minority diffusion lengths were to be measured, were lightly doped with boron to about 7 ohm-cm resistivity. All samples were deformed under compression at high temperatures (1270° to 1380°C) with varying deformation rates under a separate study using Instron and MTS machines[9-11]. During deformation, it was noted that the coarser grained and single crystal material was more susceptible to cracking under test conditions. Cracking occurred at approximately 25% strain for the coarse grained material while cracking occurred at approximately 50% strain for the fine-grained material. A summary of the samples investigated and the deformation conditions is given in Table I. This table provides details of the deformation and annealing conditions described below.

The samples were prepared for metallography by slicing into 0.5 mm sections, mounting, and polishing to 0.05 μm alumina powder with an automatic Syntron Polisher. The samples were then Sirtl etched[12] for 5 to 10 seconds.

III. RESULTS

The results of studies of these deformed samples are subdivided according to the nature of the starting material.

A. SINGLE CRYSTAL SILICON

The starting material was Czochralski-grown (001) single crystal and was dislocation free. Figure 1(a) is a photomicrograph of a typical area of (001) single crystal after deformation. Dislocations with an average density of $10^5 cm^{-2}$ were generated during the deformation process. Three separate x-ray techniques were utilized to evaluate the resulting structure and results are summarized below:

(1) Streaking of the Laue spots was observed in back-reflection x-ray Laue patterns.

(2) Only 15% of the sample was diffracted as a visible image in the Berg-Barrett test where the sample was rocked ±2.5° using a 0.25° divergent beam. The diffracted image is shown in Figure 1(b) and it is noticed that the dislocation density was too high to be resolved.

(3) Using a 3° divergent slit, a diffractomer scan gave two peaks 0.11° apart indicating two crystals.

After annealing for 10 hours, the structure shown in Figure 1(a) changed to that shown in Figure 2(a). The dislocation density in these photomicrographs is reduced to 5×10^4 cm^{-2}. The Laue x-ray topograph revealed streaking of the spots; 40% of the Berg Barrett topograph gave a visible image with the dislocation density unresolvable [Figure 2(b)]. However, the diffraction scan on these samples only indicated one peak (one crystal).

The dislocation densities of both samples are approximately the same but the lattice rotation appears to be smaller in the annealed samples. The samples experienced some recovery during anneal, but the small amount was only evident when complementary results from the various methods were obtained.

B. POLYCRYSTALLINE SILICON (CZOCHRALSKI)

The structure of Czochralski grown polysilicon prior to deformation is shown in Figure 3. Minority carrier diffusion length was measured by the surface photovoltage (SPV) method and found to be about 90 μm. Figures 4(a) and 4(b) are micrographs showing the silicon after the initial deformation and some dynamic recrystallization. These show

a grain size of about 0.2 mm with a moderately high, inhomogeneous distribution of dislocations stretching across the grain boundaries. The grains were present before the deformation had occurred (see Figure 3) and do not appear affected by the deformation. Diffusion length was reduced to 1-2 μm. Figures 5(a) and 5(b) are micrographs of a similarly deformed specimen after a 20 minute anneal at a slightly lower temperature. The structure is very similar to that of Figures 4(a) and 4(b) except that a more pronounced dislocation network appears to be forming. Diffusion length recovered only slightly to 3-4 μm. Figures 6(a) and 6(b) are micrographs of a redeformed specimen, e.g., a specimen initially deformed and annealed, then deformed again. The dislocation networks appear to have polygonized into subgrain boundaries. There is still a high density of dislocations and the grains seem to have more kinks and discontinuities. Diffusion length degraded to 0-1 μm. The last sample of this sequence is a reannealed specimen [Figures 7(a) and 7(b)]. These specimens show a more pronounced deformation structure, resulting in subgrain boundary creation and migration accompanied by high dislocation density. They do not seem to show improvement in structure after annealing comparable to that evidenced by singly deformed and annealed specimens [see Figure 5(b)]. Although the diffusion length did recover to about the same value, none of these specimens except the undeformed one would be expected to be structurally good for solar cells because of the high dislocation densities. The diffusion length measurements support this expectation. The structure appears to have degraded as more processing was performed.

C. POLYCRYSTALLINE SILICON (CHEMICAL VAPOR DEPOSITED)

The structure of polycrystalline CVD silicon supplied by Dow Corning is shown in Figure 8. Figures 9(a) and 9(b) are micrographs of a random area of a specimen after the initial deformation at ≤ 0.1 sec^{-1} and some dynamic recrystallization. (See Table I for details.) The micrographs show almost dislocation- ree recrystallized 0.5 mm grains in 70% of the material. The dislocations in the remaining 30% seem to have coalesced to form small grains of about 2.0 μm. Figure 10 is a micrograph of a specimen after a 10 minute anneal at the same temperature. The structure is very similar to that of Figure 9(a), except that 95% of the material has recrystallized. Figures 11(a) and 11(b) are micrographs of the redeformed sample showing a 1 to 2 μm grain size with high dislocation density. Remains of the prior grain boundaries can be seen in Figure 11(a), whereas in Figure 11(b) the two regions seem to be distinguished by the amount of deformation that has occurred in each of the grains. Apparently, adjacent grains do not experience equal deformation. Figures 12(a) and 12(b) show how the silicon appears after a second deformation and a 10 minute anneal. About 90% of the silicon has recrystallized leaving the grains decorated with dislocations. Again, as more processing was performed, the structure became more degraded.

Deformation at rates of 5.0 to 8.5 sec^{-1} was also performed on CVD silicon at 1380°C. Prior to deformation the CVD silicon was

annealed at 1380°C for 24 hours with no apparent change in texture[1]. Figures 13(a) and 13(b) show micrographs of two random areas of a specimen after the initial deformation. The specimen is highly deformed with very little recovery. After a 30 minute anneal, Figures 14(a) and 14(b), 50% of the specimen has recrystallized. The recrystallized regions have dislocations and twin boundaries, whereas the unrecrystallized regions seem to have formed 1 μm subgrains. After a 10 hour anneal at 1300°C, 95% of the specimen has recrystallized, Figures 15(a) and 15(b). The central regions of some recrystallized grains are decorated with dislocations and twin boundaries while a few grains appear to have nucleated dislocation-free grains and grown. Complete recrystallization does not appear to occur with reasonable (short) annealing time.

IV. DISCUSSION

The deformation of the single crystal silicon is more complex than might be expected because of the specific compression direction chosen ⟨001⟩. Single crystal silicon will normally deform by {111} ⟨110⟩ slip during uniaxial compression at high temperature (>1200°C)[13]. When a sample is deformed parallel to ⟨011⟩, the orientation is stable with respect to the deformation axis while it is not when deformed parallel to the ⟨001⟩. When the ⟨001⟩ direction is chosen for compression, deformation is accompanied by both lattice rotation and dislocation formation. If the sample is not compressed exactly in the ⟨001⟩ direction, only one slip system is active and the direction of compression rotates toward the normal to the glide plane {111} (Figure 16). The rotation overshoots the boundary between the ⟨011⟩ and ⟨100⟩ and a second slip system becomes active. If the stress is continued, the compression direction zig-zags across the boundary between the ⟨001⟩ and ⟨011⟩ until it stabilizes its compression axis on the ⟨011⟩ direction. This same type of lattice distortion occurs whether the ends of the specimen are constrained or not. The change in the direction of compression described does not occur simultaneously or uniformly over the entire crystal, so the sample displays non-uniform deformation and there is a mismatch of the planes resulting in the creation of dislocations.

A polycrystalline specimen has an additional constraint to satisfy; the matching of grain boundaries. Deformation of each grain in a polycrystalline material is dependent on grain orientation with respect to the compression axis, so the deformation process in polycrystalline samples is even more non-uniform. Dislocations will form clusters, braids, rings, loops and tangles [Figure 4(a) and 4(b)].

As expected, the observed annealing phenomena varied depending on the prior deformation and annealing temperatures. At the annealing temperatures used here, the dislocations in silicon are mobile. Dislocations glide and climb in order to annihilate each other or form lower energy configurations. The recrystallization of deformed silicon occurs by either nucleation and growth of new dislocation-free grains or by strain-induced boundary migration, i.e., migration of existing grain boundaries or of subgrain boundaries which are formed by the coalescence of dislocations. In the case of nucleation, the boundaries of the new grains will grow into the deformed grains until they impinge on each other. The resultant nucleated grains are generally free of strain and dislocations. The strain-induced boundary migration of existing grain or subgrain boundaries competes with nucleation and growth. Existing grain boundaries are either high or low angle; the subgrain boundaries are always low angle. Migrating high angle boundaries consume more of the dislocations and twins than the low angle boundaries. The central region of an existing grain is decorated by dislocations and twins if a grain boundary does not migrate through it [Figures 15(a) and 15(b)].

In the case of <001> single crystals, nucleation and growth does not occur until the sample has been compressed at least 100%[15] because subgrain boundary creation by polygonization and migration of grain boundaries occurs prior to nucleation. Recovery, in the form of dislocation annihilation and other low energy configurations, does take place during the anneal. For fine grained material (CVD), the stored energy associated with grain boundaries can be utilized in conjunction with deformation energy to aid recrystallization upon annealing.

V. SUMMARY AND CONCLUSION

From the analysis of the microstructure of deformed and annealed silicon, there is serious doubt that the structures of hot rolled silicon are consistent with high efficiency solar cells. The kinetics of silicon recrystallization are low at temperatures near the melting point (1380°C). The structure of the material appears to degrade as more processing is performed, and long anneals (10 hours) do not completely recrystallize the silicon. The resulting recrystallized grains are decorated with dislocations and twin boundaries. Recrystallization at practical rates of samples deformed 50% is only possible if the initial material has an abundance of stored internal energy, such as with CVD silicon, which can be utilized during recrystallization. If the material has a grain size of approximately 0.1 mm or greater, the stored internal energy in the material is too low for meaningful recrystallization. With such grain sizes, the amount of deformation (>>100%) necessary for practical annealing times has been shown to fracture the material during the deformation process[10]. Thus the hot rolling of silicon would require impractically large final reductions in thickness to achieve 0.1 mm grains and low dislocation density after final anneal. It must be noted that although only one sample of each deformation and anneal step was performed and the accuracy of any individual determination is low, the conclusions drawn from the sequence of steps are valid.

The investigation of the structure and diffusion length of uniaxial compressed silicon samples strongly suggests that fabrication of high efficiency solar cells by high temperature rolling of silicon is unfeasible because of requirements for excessively large deformations and long anneals to promote the otherwise sluggish recrystallization.

This paper presents results sponsored under the Low Cost Silicon Array Project at the Jet Propulsion Laboratory, California Institute of Technology, under Contract NAS 7-100, sponsored under an inter-agency agreement between Department of Energy and the National Aeronautics and Space Administration.

REFERENCES

1. Graham, C. D., Kulkarni, S., Noel, G. T., Pope, D. P., Pratt, B., and Wolf, M. 1st Quarterly Report, ERDA/JPL 954506-76/1, "Hot Forming of Silicon," June 26, 1976.

2. Socolof, S. I. and Isles, P. A., Proc 11th IEEE Photovoltaic Specialists Conference 1975, p. 56.

3. Schwuttke, G. H., Yang, K. H., and Hezel, R., Technical Progress Report No. 5, ERDA/JPL 954144-76/3 "Silicon Ribbon Growth by a Capillary Action Shaping Technique," September 15, 1976.

4. Gurtler, R. W., Baghdadi, A., Wise, J., and Ellis, R. J., Technical Quarterly Report No. 5, ERDA/JPL 954376-77/2, "Laser Zone Growth in a Ribbon-to-Robbon (RTR) Process," June 1977.

5. Wald, F. V., Third Quarterly Report, ERDA/JPL 954355-77/3, "Large Area Silicon Sheet by EFG," September 15, 1977.

6. Zook, J. D., et al., Fifth Quarterly Report, ERDA/JPL 954356-77/1, Dip Coating Process, March 31, 1977.

7. Hovel, H. J., Semiconductors and Semimetals, Volume 11, "Solar Cells," pp. 103-108, Academic Press, New York, N.Y. (1975).

8. Card, H. C. and Yang, E. S., IEEE Transactions on Election Devices, 24, (1977) 397.

9. Graham, C. D., Jr., Kulkarni, S., Noel, G. T., Pope, D. P., Pratt, B., and Wolf, M., Quarterly Report No. 2, ERDA/JPL 954506-76/2, No. 2, "Hot Forming of Silicon Sheet," September 28, 1976.

10. Graham, C. D., Jr., Kulkarni, S., Noel, G. T., Pope, D. P., and Wolf, M., Quarterly Report No. 3, ERDA/JPL 954506-77/1, "Hot Forming of Silicon Sheet," January 11, 1977.

11. Graham, C. D., Jr., Kulkarni, S., Noel, G. T., Pope, D. P., and Wolf, M., Quarterly Report No. 4, ERDA/JPL 954506-77/2, "Hot Forming of Silicon Sheet," April 21, 1977.

12. Sirtl, A. E., and Alder, A., Z. Metallk 52, (1961) 529.

13. Kelly, A. and Groves, G. W., Crystallography and Crystal Defects, p. 175, Addison Wesley, Reading, Mass., 1970.

14. Alexander, H. A. and Haasen, P., Solid State Physics, Volume 22, p. 28 ff.

15. Larson, D. C. and Kocks, U. F., Recovery and Recrystallization of Metals, Himmel, L., (Editor) p. 239, AIME and Interscience Publishers, Inc., New York, 1963.

Table I. Summary of Specimens Investigated

Sample and Figure No.	Initial Structure	Deformation and Annealing Temperature, °C	Strain Rate, (sec^{-1})	First Average Deformation, [ε]	First Time of Anneal, (min)	Second Average Deformation, [ε]	Second Time of Anneal, (min)
1	single crystal	1325	5.7	0.401			
2	single crystal	1380	5.0	0.370	600		
3	large grain polycrystalline						
4	"	1370	5.0	0.11			
5	"	1270	5.0	0.11	20		
6	"	1370	5.0	0.11	20	0.11	
7	"	1380	5.0	0.11	20	0.11	20
8	CVD polycrystalline						
9	"	1380	0.1	0.18			
10	"	1380	0.1	0.30	10		
11	"	1380	0.1	0.18	15	0.30	
12	"	1380	0.1	0.30	10	0.30	10
13	"	1340	7.4	0.516			
14	"	1380	5.0	0.186	30		
15	"	1300	8.5	0.42	600		

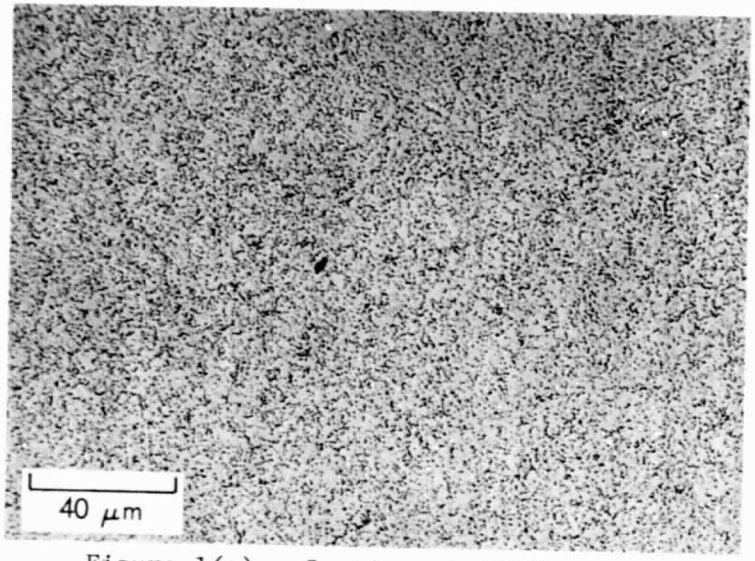

Figure 1(a). Section of (001) single crystal deformed 40.1% at 1325°C

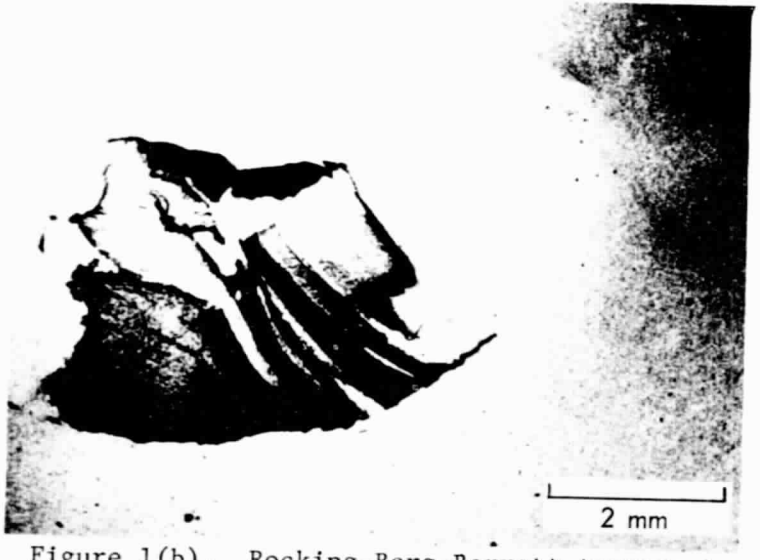

Figure 1(b). Rocking-Berg-Barrett topograph of sample in Figure 1(a)

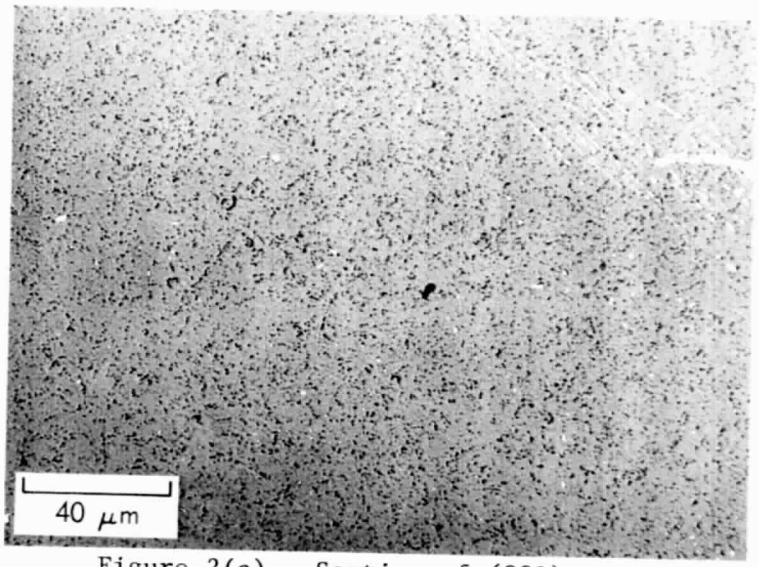

Figure 2(a). Section of (001) single crystal deformed 37% and annealed 10 hours at 1380°C

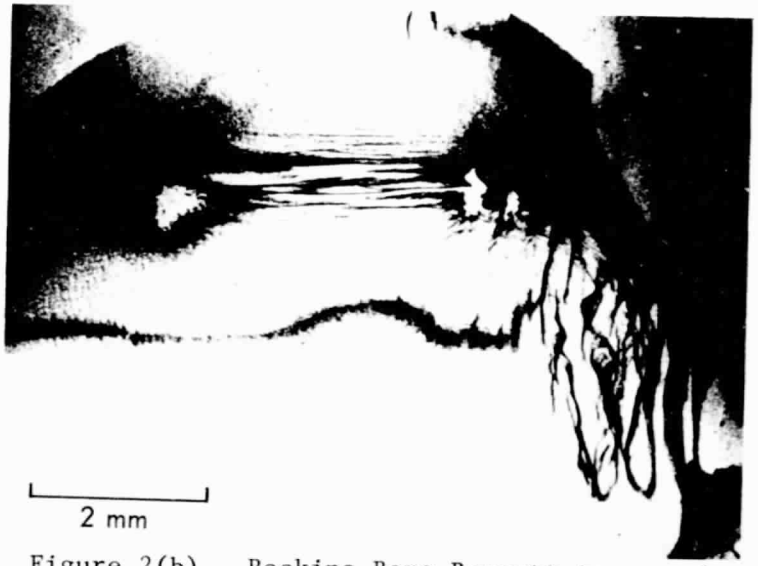

Figure 2(b). Rocking Berg-Barrett topograph of sample in Figure 2(a)

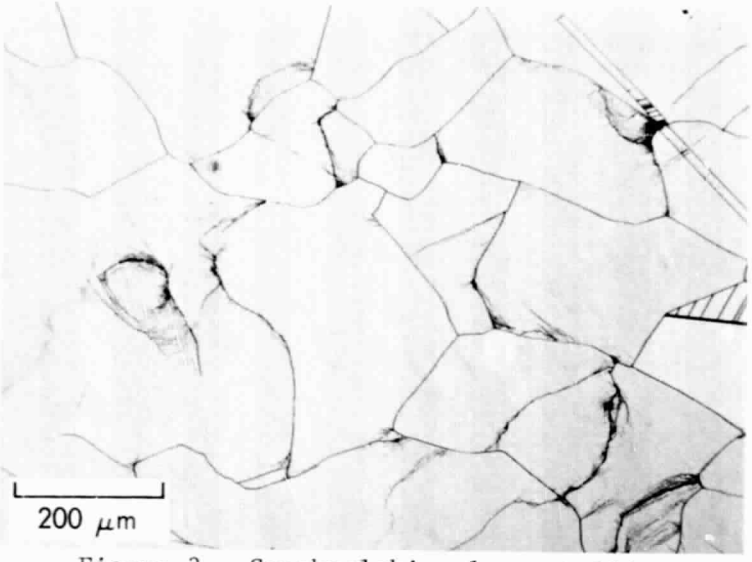

Figure 3. Czochralski polycrystalline silicon as grown, L_d ~ 90 μm

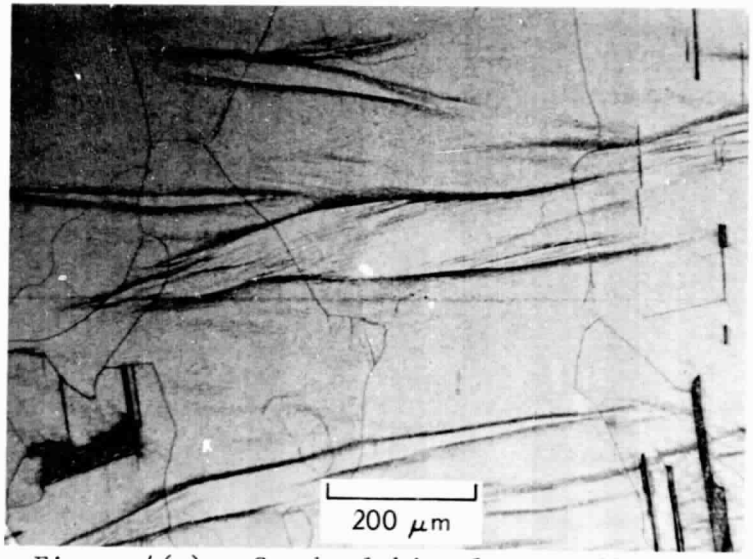

Figure 4(a). Czochralski polycrystalline silicon deformed, 11% at 1370°C, L_d ~ 1-2 μm

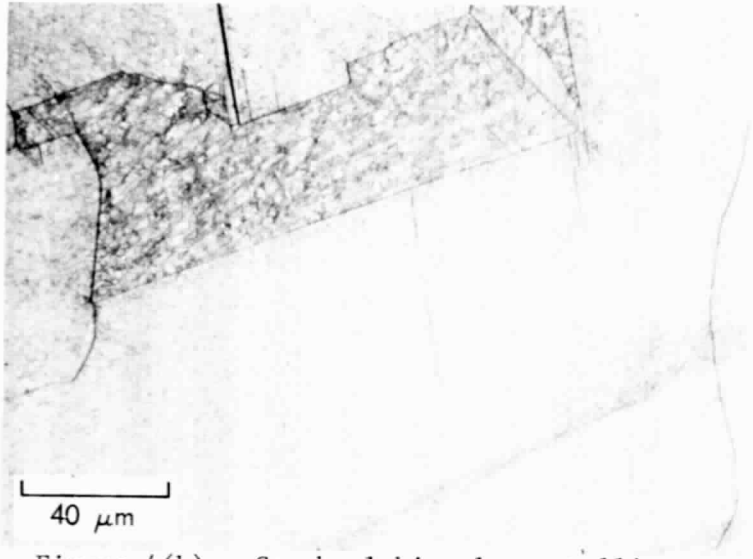

Figure 4(b). Czochralski polycrystalline silicon deformed, 11% at 1370°C, L_d ~ 1-2 μm

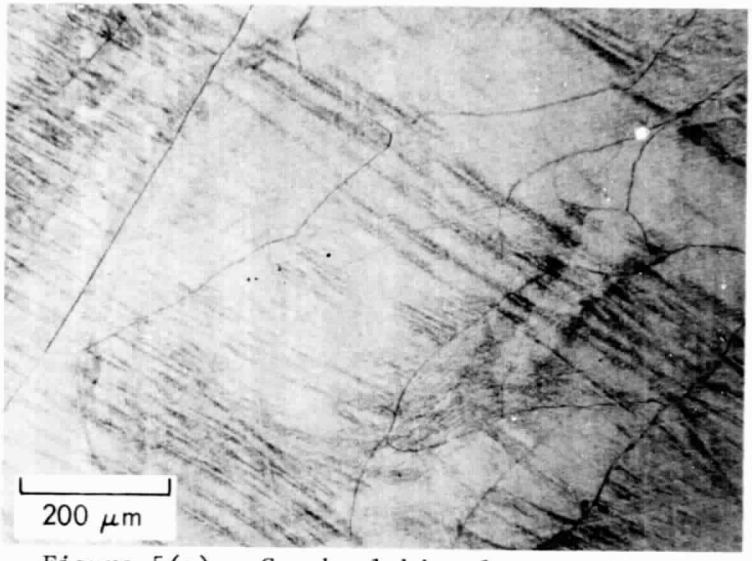

Figure 5(a). Czochralski polycrystalline silicon deformed, 11% and annealed 20 minutes @ 1270°C, L_d ~ 3-4 μm

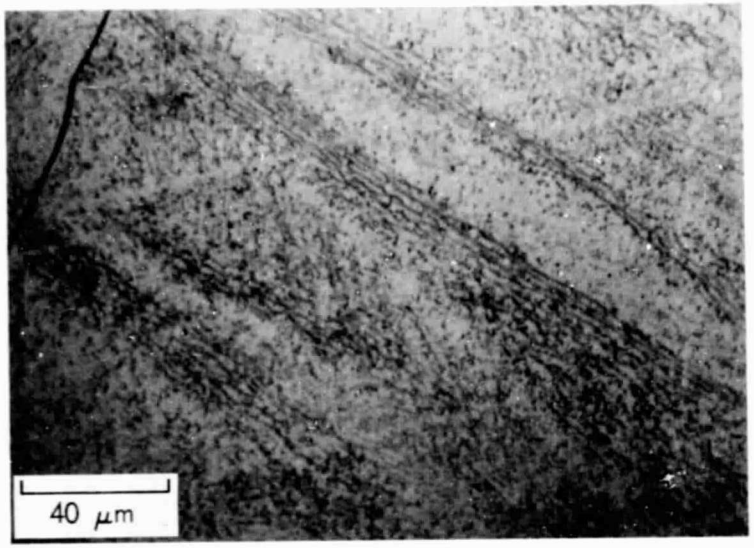

Figure 5(b). Czochralski polycrystalline silicon, deformed 11% and annealed 20 minutes @ 1270°C, L_d ~ 3-4 μm

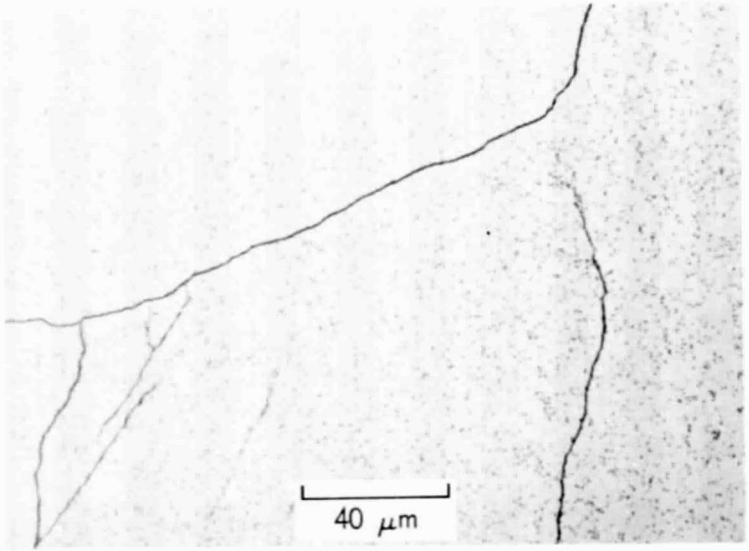

Figure 6(b). Czochralski polycrystalline silicon, deformed 11%, annealed 20 minutes and redeformed 11% @ 1370°C, L_d < 1 μm

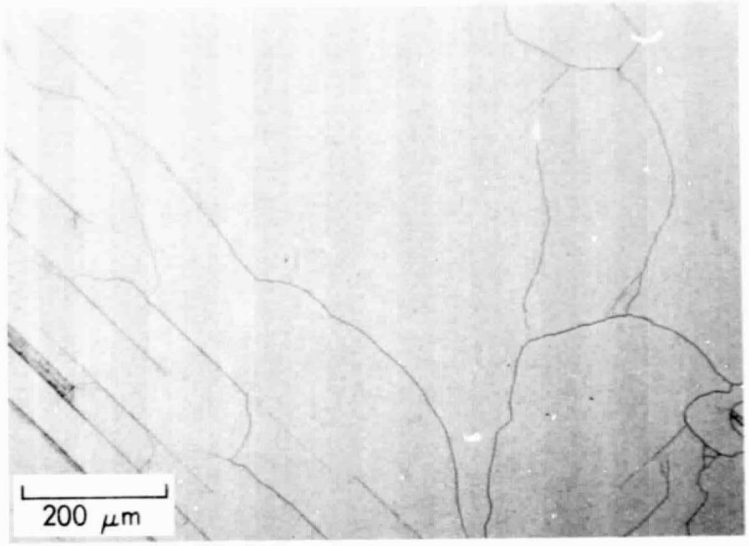

Figure 6(a). Czochralski polycrystalline silicon, deformed 11%, annealed 20 minutes and redeformed 11% @ 1370°C, L_d < 1 μm

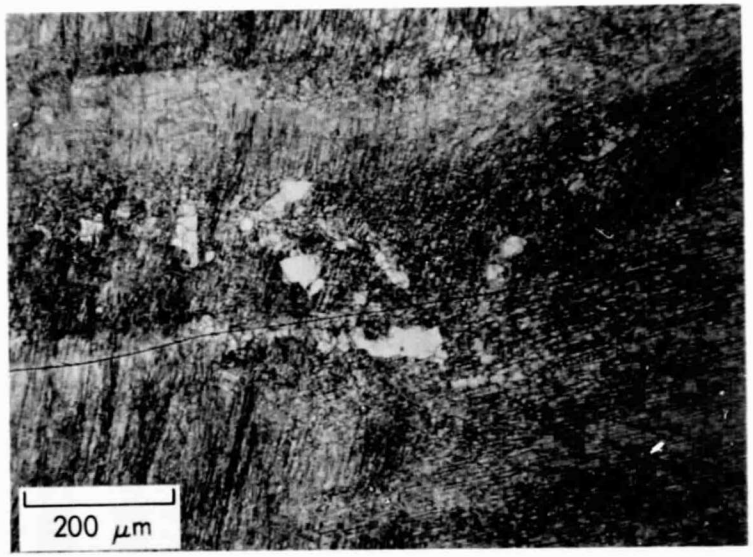

Figure 7(a). Czochralski polycrystalline silicon, deformed 11% annealed 20 minutes, redeformed 11% and reannealed 20 minutes @ 1380°C, L_d = 3-5 μm

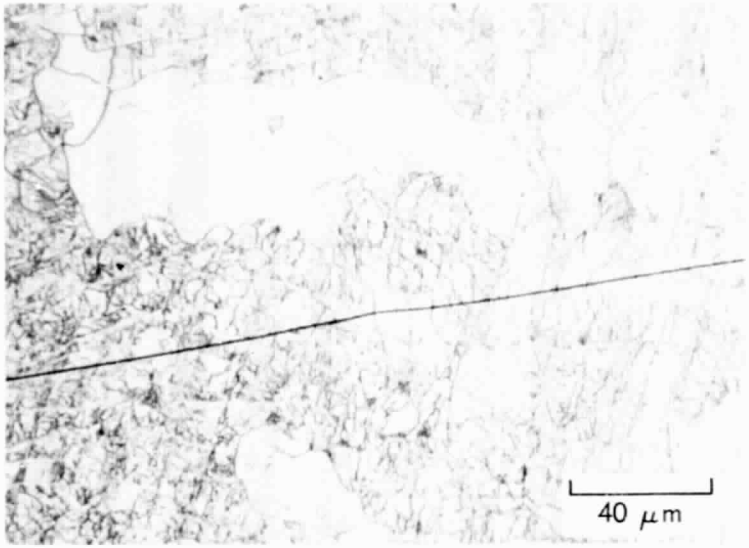

Figure 7(b). Czochralski polycrystalline silicon, deformed 11% annealed 20 minutes, redeformed 11% and reannealed 20 minutes @ 1380°C, L_d = 3-5 μm

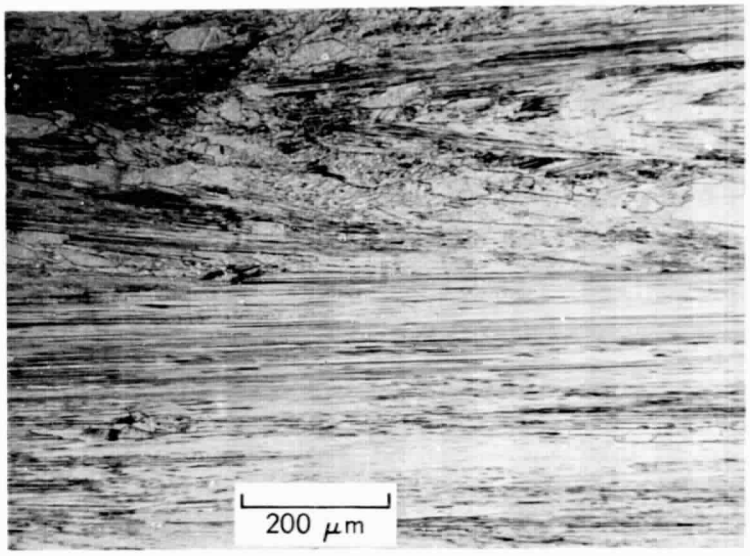

Figure 8. CVD silicon as received

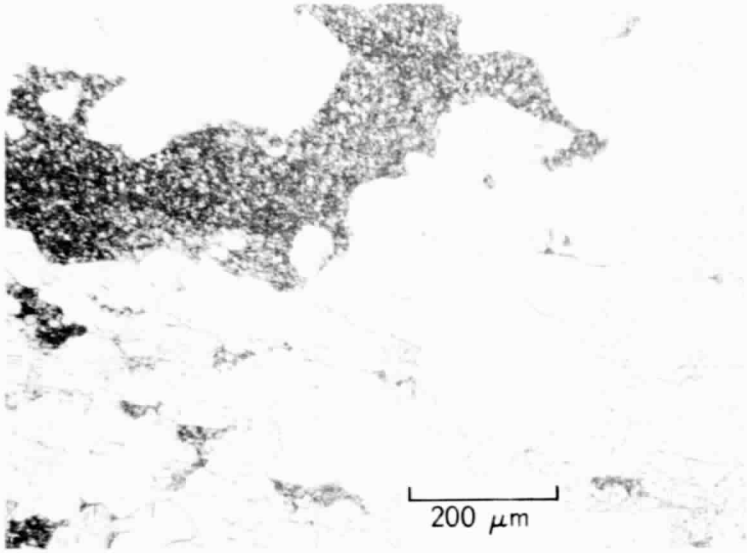

Figure 9(a). CVD silicon deformed 18% at 1380°C

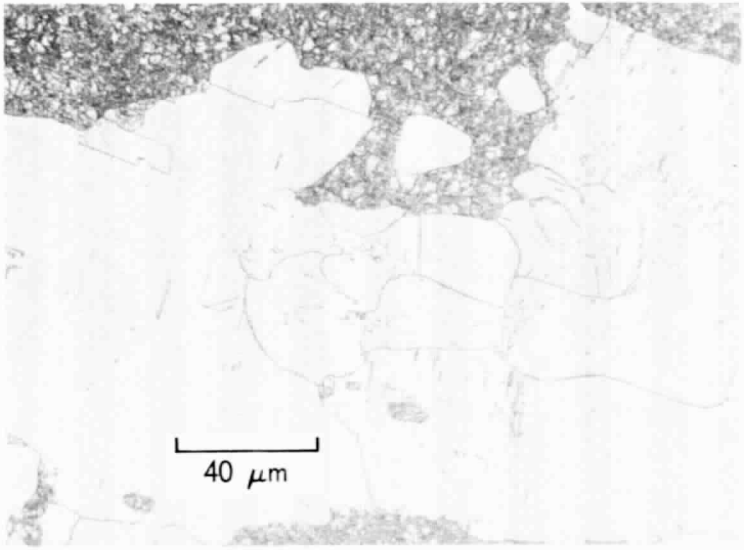

Figure 9(b). CVD silicon deformed 18% at 1380°C

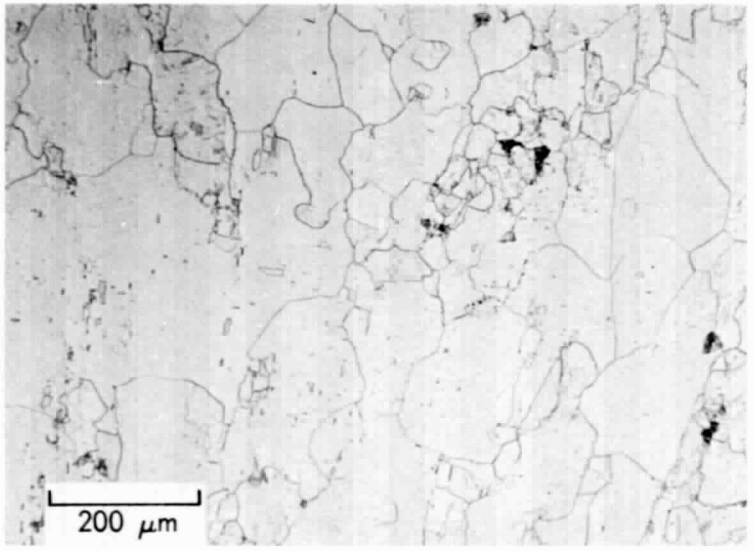

Figure 10. CVD silicon deformed 30% and annealed 10 minutes @ 1380°C

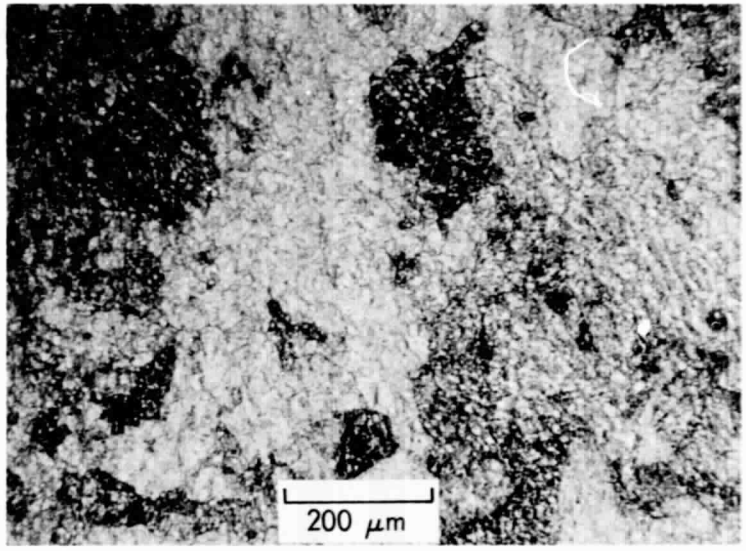

Figure 11(a). CVD silicon deformed 18% annealed 15 minutes and redeformed 30% @ 1380°C

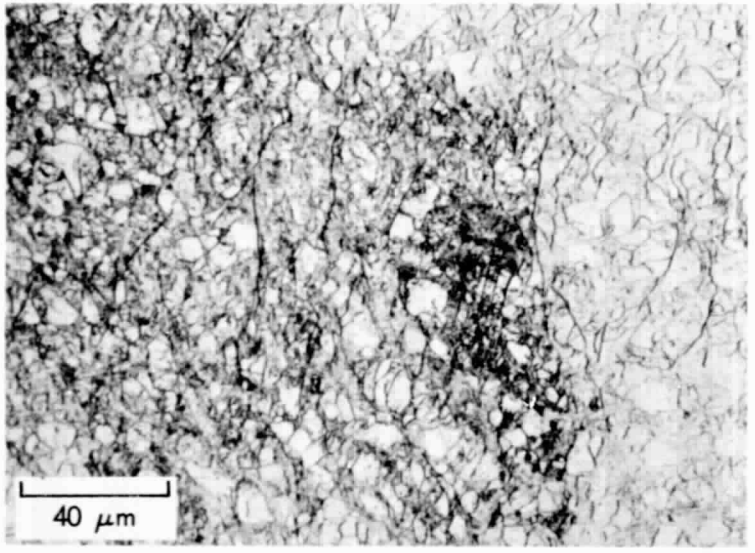

Figure 11(b). CVD silicon deformed 18% annealed 15 minutes and redeformed 30% @ 1380°C

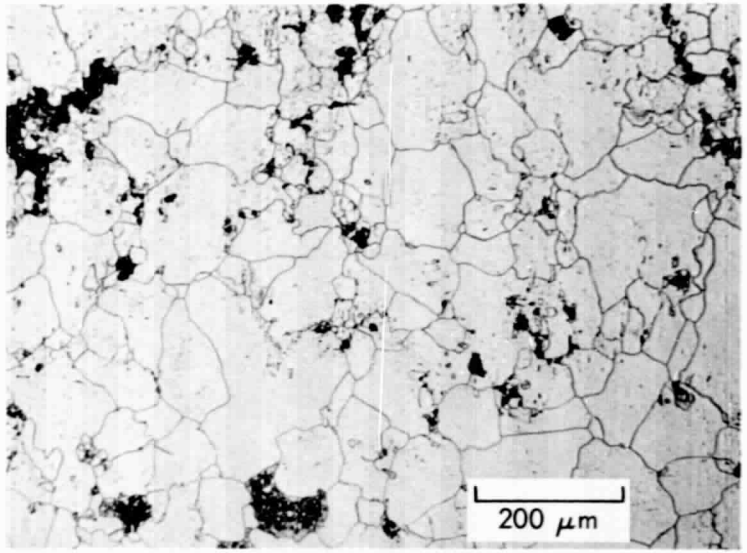

Figure 12(a). CVD silicon deformed 30% annealed 10 minutes, redeformed 30% and reannealed 10 minutes @ 1380°C

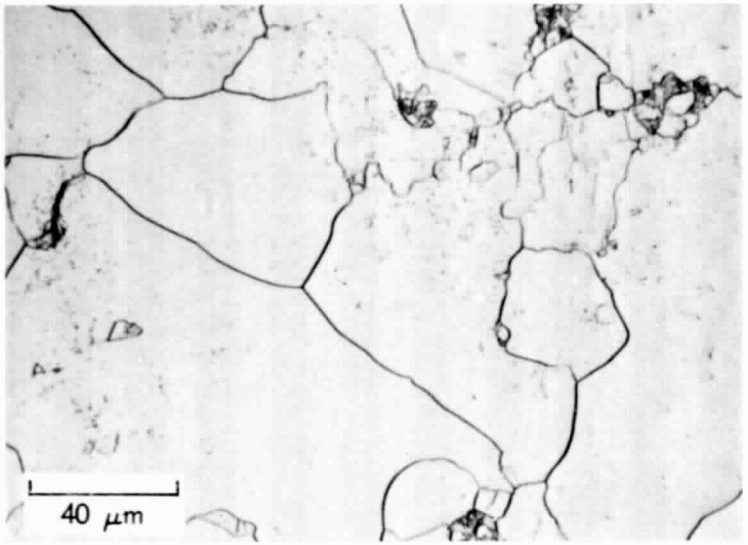

Figure 12(b). CVD silicon deformed 30% annealed 10 minutes, redeformed 30% and reannealed 10 minutes @ 1380°C

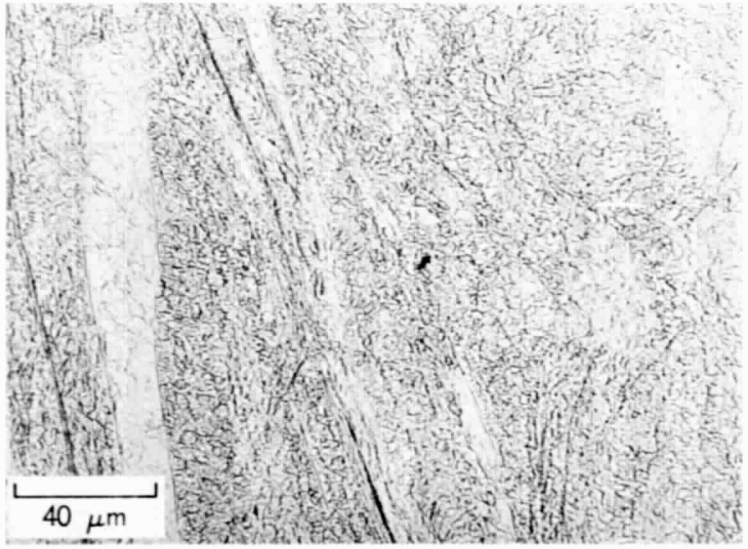

Figure 13(b). CVD silicon deformed 51.6% @ 1340°C

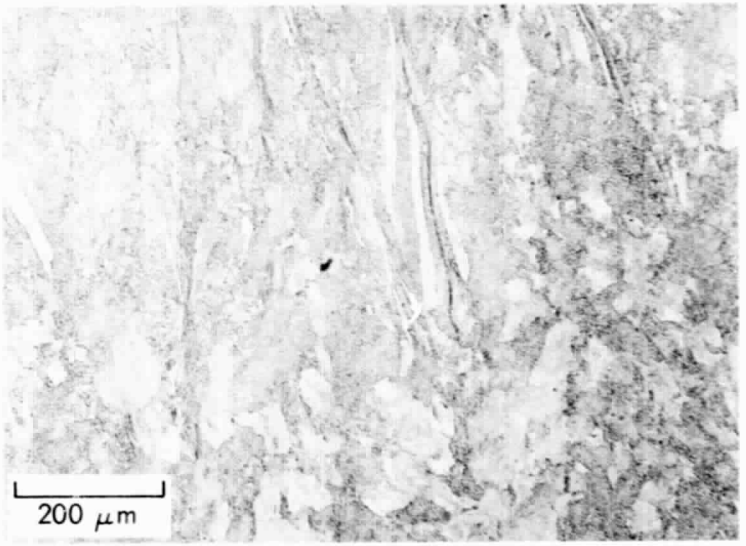

Figure 13(a). CVD silicon deformed 51.6% @ 1340°C

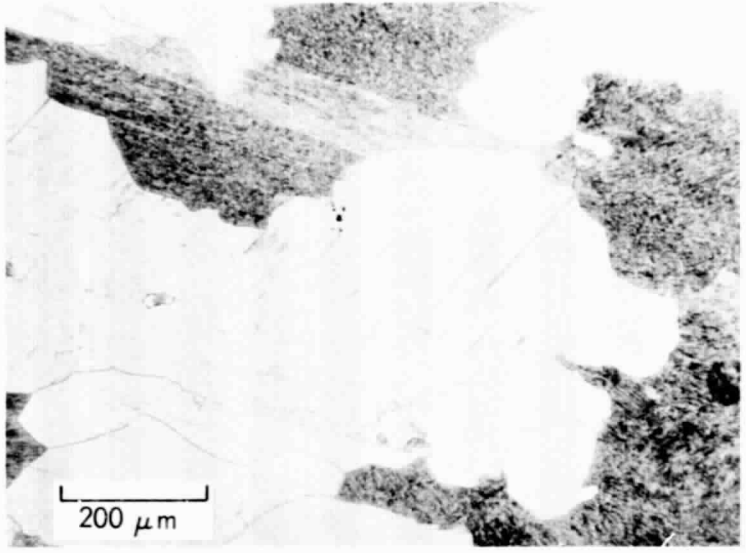

Figure 14(a). CVD silicon deformed 18.6% and annealed 30 minutes @ 1380°C

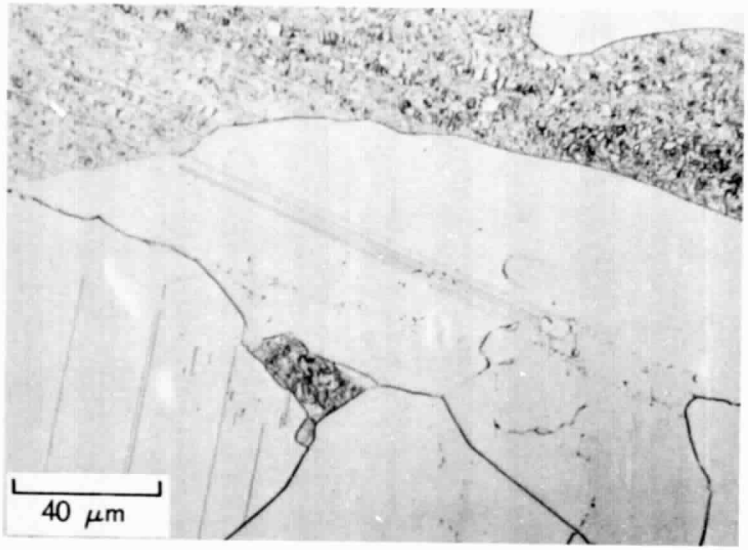

Figure 14(b). CVD silicon deformed 18.6% and annealed 30 minutes @ 1380°C

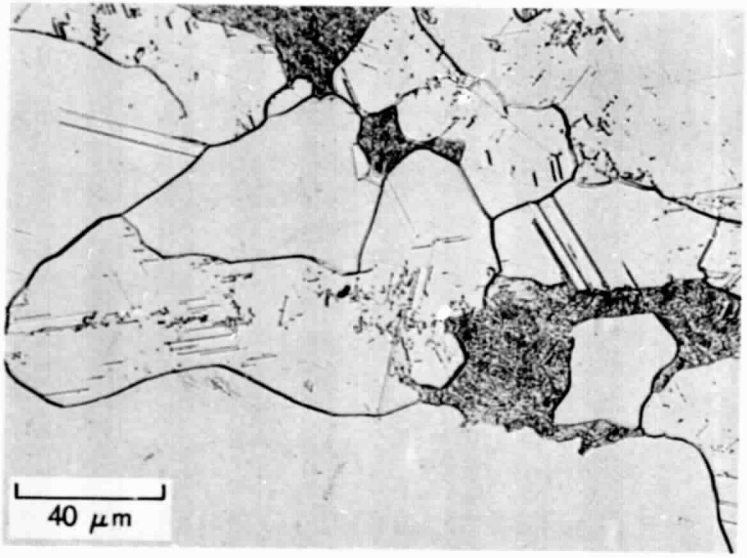

Figure 15(b). CVD silicon deformed 42% and annealed 10 hours @ 1300°C

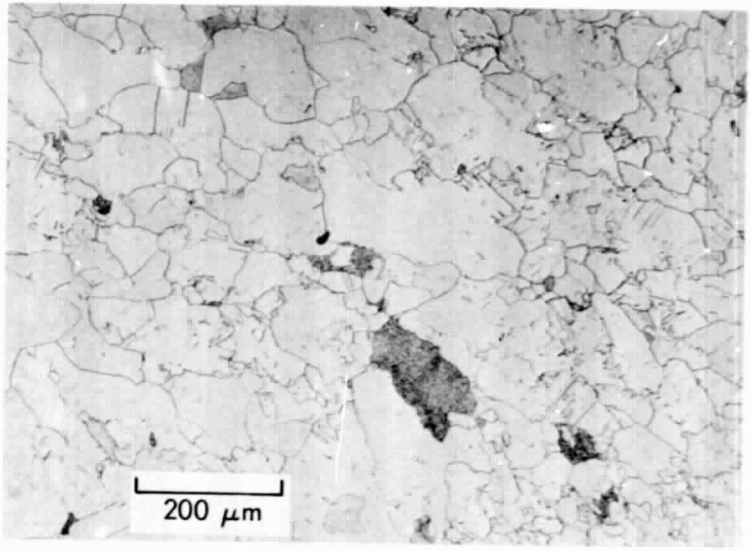

Figure 15(a). CVD silicon deformed 42% and annealed 10 hours @ 1300°C

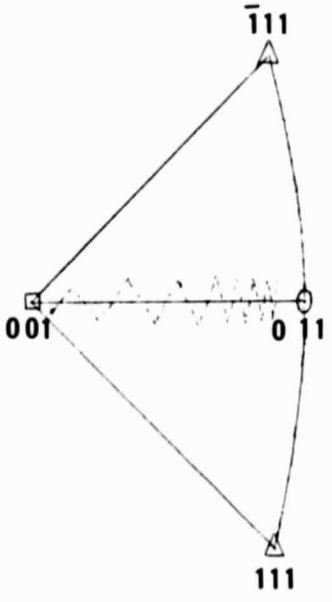

Figure 16. Changes of orientation during compression of a silicon crystal orientated close to the (001) direction